Title
Designer Heme Proteins: Achieving Novel Function with Abiological Heme Analogues

Journal
Accounts of Chemical Research, 54(24)

ISSN
0001-4842

Authors
Lemon, Christopher M
Marletta, Michael A

Publication Date
2021-12-21

DOI
10.1021/acs.accounts.1c00588

Peer reviewed

HHS Public Access

Author manuscript

Acc Chem Res. Author manuscript; available in PMC 2022 December 21.

Published in final edited form as:

Acc Chem Res. 2021 December 21; 54(24): 4565–4575. doi:10.1021/acs.accounts.1c00588.

Designer Heme Proteins: Achieving Novel Function with Abiological Heme Analogues

Christopher M. Lemon[1], **Michael A. Marletta**[1,2,3]

[1]California Institute for Quantitative Biosciences (QB3), University of California, Berkeley, Berkeley, California, 94720, United States

[2]Department of Molecular and Cell Biology, University of California, Berkeley, Berkeley, California, 94720, United States

[3]Department of Chemistry, University of California, Berkeley, Berkeley, California, 94720, United States

Conspectus

Heme proteins have proven to be a convenient platform for the development of designer proteins with novel functionalities. This is achieved by substituting the native iron porphyrin cofactor with a heme analog that possesses the desired properties. Replacing the iron center of the porphyrin with another metal provides one inroad to novel protein function. A less explored approach is substitution of the porphyrin cofactor with an alternative tetrapyrrole macrocycle or a related ligand. In general, these ligands exhibit chemical properties and reactivity that are distinct from porphyrins. While these techniques have most prominently been utilized to develop artificial metalloenzymes, there are many other applications of this methodology to problems in biochemistry, health, and medicine. Incorporation of synthetic cofactors into protein environments represents a facile way to impart water solubility and biocompatibility. It circumvents the laborious synthesis of water-soluble cofactors, which often introduces substantial charge that leads to undesired bioaccumulation. To this end, the incorporation of unnatural cofactors in heme proteins has enabled the development of designer proteins as optical oxygen sensors, MRI contrast agents, spectroscopic probes, tools to interrogate protein function, antibiotics, and fluorescent proteins.

Incorporation of an artificial cofactor is frequently accomplished by denaturing the holoprotein with removal of the heme; the refolded apoprotein is then reconstituted with the artificial cofactor. This process often results in substantial protein loss and does not necessarily guarantee that the refolded protein adopts the native structure. To circumvent these issues, our laboratory has pioneered the use of the RP523 strain of *E. coli* to incorporate artificial cofactors into heme proteins using expression-based methods. This strain lacks the ability to biosynthesize heme, and the bacterial cell wall is permeable to heme and related molecules. In this way, heme analogs supplemented in the growth media are incorporated into heme proteins. This approach can also be leveraged for the direct expression of the apoprotein for subsequent reconstitution.

Corresponding Authors: clemon@berkeley.edu; marletta@berkeley.edu.

Supporting Information: synthetic methods, compound characterization, experimental details, and numerical spectral data. This material is available free of charge via the Internet at http://pubs.acs.org.

These methodologies have been exploited to incorporate non-native cofactors into heme proteins that are resistant to harsh environmental conditions: the heme nitric oxide/oxygen binding protein (H-NOX) from *Caldanaerobacter subterraneus* (*Cs*) and the heme acquisition system protein A (HasA) from *Pseudomonas aeruginosa* (*Pa*). The exceptional stability of these proteins makes them ideal scaffolds for biomedical applications. Optical oxygen sensing has been accomplished using a phosphorescent ruthenium porphyrin as the artificial heme cofactor. Paramagnetic manganese and gadolinium porphyrins yield high-relaxivity, protein-based MRI contrast agents. A fluorescent phosphorus corrole serves as a heme analog to produce fluorescent proteins. Iron complexes of non-porphyrin cofactors bound to HasA inhibit the growth of pathogenic bacteria. Moreover, HasA can deliver a gallium phthalocyanine into the bacterial cytosol to serve as a sensitizer for photochemical sterilization. Together, these examples illustrate the potential for designer heme proteins to address burgeoning problems in the areas of health and medicine. The concepts and methodologies presented in this *Account* can be extended to the development of next-generation biomedical sensing and imaging agents to identify and quantify clinically relevant metabolites and other key disease biomarkers.

Graphical Abstract

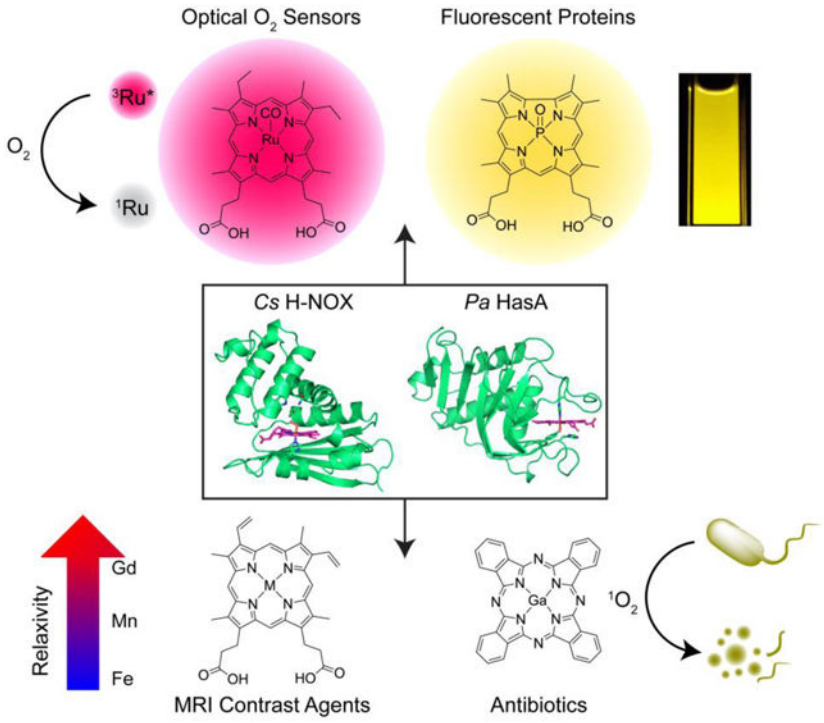

Introduction

Heme, the iron complex of protoporphyrin IX (PPIX), is an essential biological cofactor that is ubiquitous in Nature. Heme proteins have critical functions that include oxygen transport, electron transfer, and biochemical catalysis.[5] In order to interrogate the function of heme proteins, biochemists utilize a variety of techniques that include site-directed mutagenesis and the use of substrate analogs. Other protein design strategies,[6,7] such

as the incorporation of unnatural amino acids,[8,9] can provide mechanistic insight and enhance the reactivity of heme enzymes. Another powerful approach is to replace the heme cofactor with an artificial analog. This is particularly useful as a spectroscopic[10] and mechanistic[11] tool to identify the molecular details of hemoprotein function.[12] These heme analogs can bear alternative metal centers, different peripheral substituents, or even substitutions of the porphyrin core with another tetrapyrrole macrocycle or related ligand. In this way, the optical, redox, and magnetic properties, as well as chemical reactivity, can be tuned with fidelity. Consequently, this provides an inroad to develop proteins with novel reactivity or other emergent properties. While this methodology is pervasive in the field of artificial metalloenzymes,[13,14] novel protein functionality can be applied to address chemical problems in health and medicine.

De novo protein design represents another strategy to develop proteins with novel function.[15] Computational protein design goes beyond the confines of extant proteins by tailoring the structure to bind exogenous cofactors. The prototypical examples of this are protein "maquettes": α-helices that bind porphyrins and related analogs to self-assemble into four-helix bundles.[16] These maquettes can bind a variety of synthetic, abiological iron porphyrins,[17,18] zinc porphyrins and chlorins,[19] and biliverdin.[20] Modification of the protein sequence confers specificity that enables discrimination of both the metal center and peripheral substitution pattern of the cofactor.[21,22] These substituted maquettes have been utilized for a variety of applications that range from electron transfer[18] to light harvesting.[19]

In order to develop designer proteins for biomedical applications, a robust protein scaffold that is stable to harsh environmental conditions is required. An ideal platform would also tolerate point mutations to further tailor the protein for a desired application. The heme nitric oxide/oxygen binding protein (H-NOX) from the thermophilic bacterium *Caldanaerobacter subterraneus* (*Cs*), formerly classified as *Thermoanaerobacter tengcongensis* (*Tt*), meets these criteria. H-NOX proteins are bacterial gas sensors that bind diatomic gases (NO or O_2) at the heme cofactor.[23] They are homologous to the heme domain of the eukaryotic NO receptor soluble guanylate cyclase.[24,25] H-NOX proteins consist of a single domain with ~180 amino acids comprised of seven α-helices and one four-stranded antiparallel β-sheet (Figure 1a). The heme binds in a buried hydrophobic pocket that contains the heme-ligating histidine residue (H102) and a conserved Y–S–R motif that hydrogen bonds with the propionate chains of the heme cofactor. *Cs* H-NOX is an oxygen-sensing H-NOX that possesses a hydrogen bonding network (W9, N74, Y140) to stabilize the Fe(II)–O_2 adduct (Figure 1b). Gas binding at the heme cofactor results in a conformational change of the protein. This modulates the interaction between the H-NOX and its cognate signaling partner, which may be a histidine kinase, a diguanylate cyclase, or a methyl-accepting chemotaxis protein. This triggers a signaling cascade that results in a physiological response, such as flagellar motion or biofilm formation.[23]

Another heme protein that is stable to harsh environmental conditions is the heme acquisition system protein A (HasA) from the pathogenic bacterium *Pseudomonas aeruginosa* (*Pa*). Under iron-depleted stress conditions, *P. aeruginosa* secretes the apoprotein to scavenge heme from the host.[26] Apo HasA adopts an extended conformation that exposes a hydrophobic heme-binding surface (Figure 1c). Heme binding on the Y75 loop induces

closure of the H32 loop, resulting in a large-scale conformation change (Figure 1d).[27] The heme is ligated by a tyrosine (Y75) and histidine residue (H32). While Y75 and its hydrogen bonding partner H83 (Figure 1e) are highly conserved across HasA proteins, H32 is not.[28] Heme is trafficked into the bacterial cytosol through the transmembrane receptor HasR (Figure 1f).[29]

This *Account* describes the development and applications of *Cs* H-NOX and *Pa* HasA substituted with abiological heme analogs. Direct incorporation of the artificial cofactor during protein expression is accomplished using the RP523 strain of *E. coli*. This avoids the harsh conditions that are generally required to remove heme from the holoprotein and ensures that the cofactor is properly incorporated. Using this methodology, a variety of metalloporphyrins are incorporated into *Cs* H-NOX to tailor the properties of the protein for a variety of applications including optical oxygen sensors and MRI contrast agents. *Pa* HasA substituted with non-porphyrin cofactors serves as antibiotics that inhibit the growth of *P. aeruginosa*. Both *Cs* H-NOX and *Pa* HasA bind a phosphorus corrole as an inroad to novel fluorescent proteins. Together, these examples illustrate the versatility of heme proteins substituted with artificial cofactors and lay the foundation for the further development of protein-based agents to address emerging problems in health and medicine.

The RP523 Expression System

The removal and reconstitution of protein cofactors have typically been limited to robust proteins that can withstand the harsh, partially denaturing conditions required for cofactor removal. This process does not necessarily guarantee that the refolded protein adopts the native conformation. Moreover, the reconstituted cofactor may not bind at the expected site.[30,31] For example, the UV–visible absorption spectrum of *Cs* H-NOX reconstituted with a copper corrole[32] differs from expression-based incorporation (Figure 2), indicating that cofactor binding is distinct (see Supporting Information for experimental details). Together, these ambiguities call into question the integrity of reconstituted proteins.

In order to circumvent the limitations of cofactor reconstitution, our laboratory developed a generalizable methodology to incorporate heme analogs during protein expression using the RP523 strain of *E. coli*.[1] This strain was generated via mutagenesis of the C600 strain.[33] First, neomycin was used to induce a defect in respiration to yield the RP522 strain, which harbors a disruption in the *hemB* gene (δ-aminolevulinic acid (ALA) dehydratase). The RP522 strain was then mutagenized using *N*-methyl-*N*-nitro-*N*′-nitrosoguanidine to yield the heme-permeable RP523 strain, which grows on media supplemented with hemin. Although this strain does not exhibit ALA dehydratase (*hemB*) or porphobilinogen deaminase (*hemC*) activity, it does exhibit ferrochelatase activity, albeit at reduced levels (34% relative to the parent C600 strain).[33] Since the RP523 strain lacks the T7 lysogen, protein expression must be performed using an endogenous *E. coli* promoter. We have utilized the pCW vector, which is under the control of a *Taq* promoter, for reliable and robust protein expression.[1,34] In order to increase the utility of this expression system, we further engineered the RP523(DE3) strain.[12] This strain contains the λDE3 prophage, which carries the T7 RNA polymerase gene under control of the lacUV5 promoter, thereby enabling IPTG induction of the polymerase.

Since the RP523 strain grows anaerobically in the absence of heme and the cell wall is heme-permeable, we hypothesized that unnatural porphyrins could be incorporated into heme proteins during protein expression by supplementing the media with a heme analog.[1] Moreover, given the inability of RP523 cells to biosynthesize heme, heme contamination should be minimal. These hypotheses were tested by expressing mouse myoglobin (Mb) or the heme domain of the inducible isoform of nitric oxide synthase (iNOS) with manganese protoporphyrin IX (PPIX), iron mesoporphyrin IX (MPIX), or monopropargylamide (MPA) heme (Chart 1). Proteins substituted with Mn(PPIX) or Fe(MPIX) contained a near-stoichiometric amount of the porphyrin, whereas the MPA-substituted protein contained only 0.3 equivalents of the porphyrin. This result is not surprising, given the steric bulk of the propargylamide moiety and the loss of one protein–propionate interaction. HPLC analysis confirmed that no other porphyrins were present in the sample. However, a small amount (<5%) of Fe(PPIX) contamination was observed in the case of Mn(PPIX)-substituted iNOS; this could be mitigated by limiting the growth time after the induction of protein expression. These proteins exhibited the expected UV–vis spectra and gas binding properties (NO, CO, O_2). Moreover, the Fe(MPIX)-substituted iNOS was catalytically competent. Together, these results demonstrate that the porphyrin cofactors were properly incorporated.[1] This method has also successfully been applied to the incorporation of Zn(MPIX) and Pd(MPIX) in *Cs* H-NOX.[34] Proteins expressed with manganese or zinc porphyrins exhibit slight contamination with the corresponding Fe complex. The media could be supplemented with higher porphyrin concentrations and/or a salt of the appropriate metal to reduce iron contamination. The origin of trace iron impurities could be promiscuous ferrochelatase activity, where the enzyme replaces the porphyrin-bound metal with iron from the growth medium. This hypothesis is consistent with the observation that supplementation with an appropriate metal salt abrogates iron contamination.

Expression-based methods using the RP523 strain can be leveraged to incorporate synthetic or semi-synthetic cofactors. Heme can be directly modified to add a *meso*-alkyne substituent,[35] a versatile synthon for further chemical modification. It was found that the triisopropylsilyl-protected alkyne (Chart 1, R = TIPS) was readily incorporated into *Cs* H-NOX, indicating that this bulky, hydrophobic cofactor crosses the bacterial cell wall. Moreover, the substituted protein exhibits the expected gas binding properties (NO, CO, O_2), demonstrating that the cofactor is properly incorporated. Expression with the deprotected alkyne (Chart 1, R = H) enabled fluorescent labeling of *Cs* H-NOX with an azide-functionalized dye.[35]

A true generalization of our expression-based method would be to demonstrate that non-porphyrin cofactors, such as corroles, could be incorporated into heme proteins. Corroles, like porphyrins, are tetrapyrrole macrocycles, but possess a contracted 23-atom core.[36] Despite their similar structure, corroles exhibit chemical reactivity, optical properties, and electronic structures distinct from porphyrins.[37,38] The unique photophysical[39] and photochemical[40] properties of corroles have been leveraged for a variety of applications.[41] An appropriately functionalized copper corrole (Chart 1) crosses the RP523 cell wall and is incorporated into *Cs* H-NOX (Figure 2). In cases where the amount of cofactor is limited, we have developed a reliable method for small-scale (1 L) anaerobic expression (see Supporting Information). An extension of the RP523 methodology can be utilized to

directly express the apoprotein, thereby avoiding the harsh conditions necessary for heme removal. This is advantageous for incorporating cofactors that cannot cross the bacterial cell wall.[4]

For expression-based incorporation of artificial heme analogs using the RP523 strain, an anaerobic starter culture is used to inoculate a fermenter vessel containing nitrogen-sparged media. The culture is grown at 37 °C to reach a suitable optical density (OD_{600} = 0.4–0.6), and then the culture is cooled to the temperature used for protein expression (*e.g.*, 18 °C). After the culture has reached the desired temperature and the OD_{600} = 0.6–0.8, the heme analog is added (5–10 mg/L of culture) as a DMSO solution just prior to inducing protein expression. After 16–24 hours of growth, the cells are harvested then lysed using a high-pressure homogenizer. Purification is performed using Ni affinity chromatography followed by ion exchange and/or size exclusion chromatography as necessary. Protein yields are dependent on the nature of the protein, the expression vector, and the exogenous heme analog. Detailed methods are provided in the Supporting Information for *Cs* H-NOX substituted with the Cu corrole reported herein.

Other expression-based methods have been reported for the incorporation of unnatural porphyrin cofactors. *Enterococcus faecalis* was utilized to express catalase substituted with various metalloporphyrins. HPLC analysis of some derivatives exhibited complex chromatograms, indicating that bacterial modification of the porphyrin can occur.[42] Another approach is to co-express the outer-membrane heme transporter ChuA with the protein of interest.[43] The BL21(DE3) strain of *E. coli*. can biosynthesize Co(PPIX) and subsequently incorporate it into a variety of heme proteins.[44] In contrast to these methods, the RP523 expression system does not rely on bacterial systems to acquire or synthesize the cofactor, enabling precise tuning of heme proteins for a variety of applications.

Optical Oxygen Sensors

The concentration of molecular oxygen is a critical parameter for all forms aerobic of life. Organisms from bacteria to mammals have complex cellular machinery to detect and respond to changes in oxygen concentration. While several modalities have been developed for biological oxygen sensing,[45] phosphorescence quenching is non-invasive and offers high spatial resolution (<1 μm). A sensor molecule in a triplet excited state undergoes collisional quenching with O_2, returning the sensor to the ground state. Both Pd(II) and Pt(II) porphyrins are well-known O_2 sensors that exhibit long-lived phosphorescence (650–800 nm) that is responsive to O_2 at biologically-relevant concentrations.[46,47] Since these porphyrins are insoluble in water, incorporation into heme proteins represents a facile means of imparting water solubility.[48,49,50]

Our laboratory developed oxygen sensors where Ru(CO)(MPIX) was incorporated into either *Cs* H-NOX or myoglobin.[2] The RP523 expression system yielded protein with a stoichiometric amount of the porphyrin. A crystal structure of the Ru-substituted H-NOX revealed that the porphyrin is bound to the protein akin to the native heme cofactor. The Ru center coordinates to the proximal histidine residue (H102) and the axial CO ligand hydrogen bonds with the O_2-stabilizing tyrosine residue (Y140) (Figure 3a). Moreover, the

protein fold is nearly identical to the native, heme-bound structure with a root-mean-square (RMS) deviation of 1.3 Å. Together, these results indicate that Ru(CO)(MPIX) is properly incorporated into *Cs* H-NOX.[2]

The Ru-substituted proteins exhibit a phosphorescence transition around 665 nm with a quantum yield (in the absence of O_2) of 0.017% and 0.0048% for H-NOX and myoglobin, respectively. It is noteworthy that the protein environment has a significant influence on the photophysical properties of the porphyrin. H-NOX confers a 3.5-fold enhancement in quantum yield relative to myoglobin. Stark differences are also observed for the phosphorescence lifetime in the absence of O_2: 7.7 μs for H-NOX and 37.3 μs for myoglobin. Under ambient O_2, the lifetimes are quenched to 2.9 μs and 12.2 μs; these values are 38% and 33% of the unquenched lifetime. Despite the differences in lifetime and quantum yield, the Ru porphyrin exhibits similar oxygen sensitivity in both proteins. The lifetime of the H-NOX sensor was measured at various oxygen concentrations, and the response was linear over the 0 to 256 μM O_2 range, exhibiting a bimolecular quenching constant of 8.2×10^8 M^{-1} s^{-1} (Figure 3b). Despite the low quantum yield, Ru-substituted H-NOX is a sensitive sensor at biologically relevant oxygen concentrations.

To improve upon the Ru-based sensor, we are currently developing H-NOX-based sensors that utilize Pd(MPIX) or Pt(MPIX), since these metalloporphyrins exhibit significantly higher phosphorescence quantum yields. Additionally, we are incorporating a second, oxygen-insensitive fluorophore to furnish a ratiometric sensor with two-color emission. By incorporating two emissive species into the sensor construct, oxygen can be quantified by the emission intensity ratio of the two components. This is a robust sensing methodology that is independent of sensor concentration and is functional in cells and tissues.[51]

MRI Contrast Agents

Magnetic resonance imaging (MRI) is a noninvasive imaging technique with sufficiently high spatial resolution (~mm) to differentiate soft tissues. The signal for this technique stems from the longitudinal ($1/T_1$) and transverse ($1/T_2$) relaxation rates of water protons. Contrast agents are paramagnetic molecules that increase the relaxation rates of water protons in the vicinity of the molecule, thereby increasing the contrast of the image. The enhancement in the relaxation rates is known as relaxivity; r_1 and r_2 refer to the increase in $1/T_1$ and $1/T_2$, respectively.[52] There are several parameters that govern the relaxivity of a contrast agent including: the electron spin quantum number of the metal (S), the number of bound water molecules (q), and the rotation speed (or tumbling rate) of the molecule.[53] Relaxivity of an MRI contrast agent is enhanced by increasing S and q and decreasing the tumbling rate (*i.e.*, increasing the molecular weight) of the molecule.

To enhance the relaxivity of metalloporphyrins, we incorporated a variety of porphyrins into *Cs* H-NOX.[3] It was expected that encapsulation of the porphyrin in a protein environment would substantially decrease the tumbling rate to increase relaxivity. First, Fe(III)(PPIX) was compared for myoglobin and *Cs* H-NOX to assess the effect of different protein environments. H-NOX exhibited significantly higher relaxivities than myoglobin (Figure 4). To further enhance relaxivity, other paramagnetic porphyrins were substituted into

Cs H-NOX. Expression-based incorporation with the RP523 strain was used to prepare Mn(PPIX)-substituted H-NOX. The protein was isolated as the Mn(III) complex, but could readily be reduced to the Mn(II) derivative. The Mn(III) species exhibits higher relaxivities than the Mn(II) complex. Since Gd(III) is the prototypical metal used for MRI contrast agents, Gd(MPIX) was also incorporated into *Cs* H-NOX via reconstitution of the apoprotein. This protein exhibited superior relaxivities (r_1 = 28.7 mM^{-1} s^{-1} and r_2 = 39.9 mM^{-1} s^{-1}) that are nearly 10 times higher than commercial, clinically-approved small-molecule Gd(III) chelates ($r_1 \sim r_2 \sim$ 3–4 mM^{-1} s^{-1}).[52] These results indicate that *Cs* H-NOX provides an exceptional platform for the development of MRI contrast agents.

While MRI is generally utilized as an imaging technique, it can also be exploited as a sensing modality. Derivatives of BM3h were engineered to modulate r_1 in response to arachidonic acid.[43] The protein was expressed using ChuA-expressing BL21 *E. coli* to incorporate Fe(PPIX) or Mn(PPIX). The Mn(III)-substituted protein exhibited higher r_1 relaxivity than the Fe(III) complex. Titrations of the WT Mn-substituted protein with arachidonic acid exhibited optical changes, but only a nominal change in r_1. Directed evolution of BM3h[54] and chimeric BM3h homologues[55] yielded protein variants with enhanced optical and magnetic responses to arachidonic acid. The Mn-substituted chimeric variant C1634 exhibited the highest relaxivity and greatest response to arachidonic acid.[43] This study demonstrates that a combination of protein engineering techniques can yield designer proteins for advanced biomedical applications.

Antibiotics

One escalating global health crisis is antibiotic resistance, which has been precipitated by the overuse and inappropriate prescribing of antibiotics.[56] The limited availability of novel antibiotics has exacerbated the problem. Traditional antibiotics target bacterial DNA synthesis, the ribosome, or the cell wall. Bacteria are adept at overcoming the toxicity caused by these drugs.[57] Modern antibiotic drug discovery aims to identify new targets (*e.g.*, virulence factors, toxin production, or nutrient acquisition)[58] and exploit mechanisms of action that are not susceptible to existing modes of drug resistance.[59]

One strategy is to restrict bacterial iron acquisition, as it is an essential nutrient for invading pathogens.[60] Interfering with the heme acquisition system (Has) of pathogenic bacteria represents one approach to novel antibiotics. A variety of macrocyclic iron cofactors (Fe(PPIX), Fe(MPIX), Fe(OEP), Fe salophen, Fe phthalocyanine, Chart 1) were reconstituted into *Pa* HasA and the effect on bacterial growth inhibition was examined.[61] Crystal structures of HasA substituted with Fe(MPIX), Fe salophen, or Fe phthalocyanine were obtained and revealed that the iron complexes were ligated by H32 and Y75, analogous to heme. Moreover, the overall fold of the protein is nearly identical to the native heme-bound protein, with RMS deviations of 0.443 Å, 0.810 Å, and 0.915 Å for Fe(MPIX), Fe salophen, and Fe phthalocyanine, respectively. These results indicate that these heme analogs are properly incorporated into HasA.[61] The successful reconstitution likely stems from the fact that the apoprotein exhibits an extended conformation and natively binds a planar, hydrophobic iron complex.

To test the effect on bacterial growth, *P. aeruginosa* was grown in the presence of HasA pre-loaded with these iron complexes. It should be noted that EDTA was added to the growth medium to scavenge free iron; bacteria did not grow under this condition. Bacteria grew in the presence of HasA bound to Fe(PPIX) or Fe(MPIX), but not Fe salophen or Fe phthalocyanine (as indicated by the optical density at 600 nm, OD_{600}) (Figure 5a). Next, *P. aeruginosa* was grown in the presence of both heme-bound HasA (as a useable iron source) and Fe salophen or Fe phthalocyanine substituted HasA. While the bacteria grew in the presence of Fe salophen-substituted HasA, no growth was observed for HasA bound to Fe phthalocyanine, despite the presence of heme-loaded HasA in the growth medium (Figure 5b). This indicates that HasA with Fe phthalocyanine inhibits heme acquisition (IC_{50} = 24 nM). When other iron sources are available (trace iron in the growth medium or heme supplementation), HasA bound to Fe phthalocyanine did not inhibit bacterial growth. Perhaps the HasA–HasR complex (Figure 1f) with Fe phthalocyanine is so tight that HasA does not dissociate, preventing further acquisition of iron. Alternatively, the phthalocyanine may be transferred to HasR, but the macrocycle could block the channel to prevent heme acqusition.[61]

The ability of HasA to bind non-heme cofactors can be leveraged for additional antibiotic strategies, such as photochemical sterilization. HasA was utilized to deliver a Ga phthalocyanine into the bacterial cytosol.[62] This cofactor serves as a photosensitizer to generate singlet O_2 to kill bacteria. Apo HasA was reconstituted with Ga phthalocyanine and a crystal structure revealed that the Ga(III) center is ligated by H32 and Y75 and the protein exhibits the same fold as the native holoprotein (RMS deviation of 0.71 Å). Cultures of *P. aeruginosa* treated with the substituted HasA and irradiated with light killed >99.99% of the bacteria, while a *hasR* knockout strain was not affected. Fluorescence microscopy confirmed the presence of phthalocyanine in the cytosol, indicating that the HasA/HasR system was able to transport this cofactor. Ga phthalocyanine substituted HasA can also photodynamically inactivate multidrug-resistant *P. aeruginosa*, as well as bacteria that have high HasR sequence homology to *P. aeruginosa* (*e.g.*, *Pseudomonas protegens,* 75% sequence homology).[62] A similar strategy exploited the HasA/HasR system of *P. aeruginosa* to transport a Ga salophen, which inhibits transcription of the *has* operon and blocks iron uptake through xenosiderophore receptors.[63] Together, these studies demonstrate that HasA can be utilized to deliver heme analogs into the bacterial cytosol.

Fluorescent Proteins

Since the discovery of green fluorescent protein, the field of fluorescent proteins has greatly expanded, demonstrating their use as *in vivo* tags, sensitizers, and sensors.[64] Various design strategies have tuned protein emission from ultraviolet to near-infrared (NIR) wavelengths. For *in vivo* applications, red or NIR light (600–1100 nm) is preferred because tissue is transparent to these wavelengths.[65] However, fluorescent proteins that emit in this spectral range are notoriously weak (Figure 6),[66] limiting their use for *in vivo* applications. Additionally, fluorescent proteins typically have broad emission profiles that can span over 200 nm, complicating multicolor imaging and ratiometric sensing.

To improve upon the optical properties of traditional fluorescent proteins, we developed a strategy to incorporate fluorescent heme analogs into stable protein scaffolds. We incorporated a phosphorus corrole (Chart 1) into both *Cs* H-NOX and *Pa* HasA.[4] Corroles exhibit red-shifted emission profiles and higher quantum yields than porphyrins.[67] While we initially targeted red fluorescent Ga(III) and Al(III) complexes, the corrole ligand was too electron-rich to enable the isolation of these molecules. The photostable P(V)=O derivative was synthesized in high yield, but exhibited yellow-orange emission with a lower-than-expected fluorescence quantum yield (ϕ_f). Using the RP523 expression system, only a trace amount of the P(V)=O corrole was incorporated into *Cs* H-NOX, indicating that this molecule does not cross the bacterial cell wall. Direct expression of the apoprotein was performed using the RP523 system, circumventing the need for heme removal. Reconstitution of apo H-NOX and HasA with the phosphorus corrole resulted in high cofactor incorporation (> 96%) (Figure 7). When stored at 4 °C protected from light, these conjugates are very stable, exhibiting nominal corrole loss after two months. The absorption spectra of the reconstituted proteins are distinct from the free corrole in buffer, indicating the corrole is bound in a hydrophobic environment. Corrole fluorescence is enhanced upon protein binding: ϕ_f = 2.5% for H-NOX, 7.3% for HasA, and 1.2% for the unbound corrole. Unlike traditional fluorescent proteins, the main fluorescence transition is concentrated in a sharp band, offering an advantage over traditional fluorescent proteins.[4]

While previous studies of *Cs* H-NOX and *Pa* HasA demonstrated that the artificial cofactors bind analogous to heme (*vide supra*), it was unclear if this would be the case for the P(V)=O corrole. In solution, this corrole does not bind to histidine and remains a five-coordinate species. DFT calculations corroborate that imidazole binding is destabilizing.[4] Given that histidine residues are integral to the heme binding pocket of both *Cs* H-NOX and *Pa* HasA, it was unknown how the corrole binds to these proteins. To elucidate the corrole–protein interactions, a series of point mutants were generated to modulate the heme binding pocket and identify critical contacts.[68] In the case of H-NOX, changes in the distal hydrogen-bonding network (W9F and Y140F) had no effect on corrole binding, indicating that the P=O unit does not interact with these residues. Consequently, the distal subdomain is likely shifted away from the heme binding pocket, akin to the unliganded protein.[69] Removal of the heme-ligating histidine residue (H102) or P115 significantly decreases corrole binding, indicating that these residues are critical. Molecular dynamics simulations identified that H102 and P115 are tightly coupled, underscoring the importance of both residues. The P=O unit hydrogen bonds to H102 and this serves as the primary protein–corrole interaction. On the basis of the unliganded crystal structure, the imine nitrogen of the H102 side chain could form a hydrogen bond with the backbone carbonyl of P115. Results indicate that H102 is protonated under the experimental conditions at pH 6.5. Consequently, protonated H102 can hydrogen bond to both the P=O unit of the corrole and P115. This additional interaction rigidifies the heme binding pocket to enhance corrole binding, and accounts for the necessity of both residues (Figure 8a).[68]

In the case of HasA, modulation of the H32 loop had no effect on corrole binding, but variation of the Y75 loop had a profound effect. The Y75F variant decreased corrole binding by ~50%, but no corrole binding was observed for H83 variants, indicating that this residue is essential. pH-dependent emission studies indicate that H83 is protonated under

the experimental conditions at pH 6.5 In order to determine the conformation of the protein, cysteine variants were labeled with fluorescein maleimide and Förster resonance energy transfer (FRET) was utilized to determine the fluorescein–corrole distance. The FRET analysis revealed that the protein adopts an extended, apo-like conformation. Together, these results indicate that the corrole binds to the Y75 loop and the P=O unit primarily hydrogen bonds with protonated H83 and, to a lesser extent, Y75 (Figure 8b). This hydrogen bonding network may also include water and/or buffer molecules to further stabilize corrole binding. A docking model generated from the apo HasA crystal structure and the DFT-optimized geometry of the phosphorous corrole (Figure 8c) is consistent with the FRET analysis.[68]

These examples illustrate that unnatural heme analogs can bind to proteins in unexpected ways. This underscores the need to identify these interactions and ensure proper protein folding and cofactor incorporation, especially in cases of reconstitution.

Summary and Outlook

The RP523 *E. coli* expression system is a facile way to incorporate unnatural porphyrins into heme proteins. An expression-based system ensures that the protein is properly folded and the cofactor is correctly bound, thereby avoiding the ambiguities of protein reconstitution. Unlike other expression methods, the permeability of the RP523 cell wall allows a variety of substituted porphyrins, and even corroles, to be incorporated into heme proteins. Since this system does not rely on bacterial machinery for cofactor synthesis or uptake, the scope of peripheral substitution and metal incorporation is not limited. The RP523 methodology can also be used for the direct expression of the apoprotein, circumventing the harsh conditions necessary for heme removal.

Substitution of heme proteins with abiological analogs enables the tuning of optical, redox, and magnetic properties to furnish novel proteins with designer functions. While this approach has been popularized for the development of artificial metalloenzymes, it has also been utilized for a variety of biomedical applications. The use of stable protein scaffolds, namely *Cs* H-NOX and *Pa* HasA, has enabled the development of optical oxygen sensors, MRI contrast agents, novel antibiotics, and fluorescent proteins. H-NOX substituted with Ru(CO)(MPIX) is a sensitive oxygen sensor at biologically-relevant oxygen concentrations. Incorporating Mn(III)(PPIX) and Gd(III)(MPIX) into H-NOX yields high-relaxivity MRI contrast agents that are superior to clinically-used small-molecule Gd(III) chelates. An Fe phthalocyanine bound to HasA inhibits the growth of *Pseudomonas aeruginosa*. Additionally, the HasA/HasR system can be utilized to transport hydrophobic heme analogs across the bacterial cell wall. Finally, incorporation of a fluorescent phosphorus corrole in H-NOX and HasA yields yellow-orange emitting proteins that offer advantages over traditional fluorescent proteins. The P=O corrole–protein interaction is a rare example where the binding mode of the artificial cofactor is distinct from heme.

The examples outlined in this *Account* represent just the beginning of the possible applications that can be leveraged with substituted heme proteins. While fluorescent H-NOX proteins and MRI contrast agents are amenable for imaging applications, they could serve as platforms for sensor development by including an analyte-specific recognition element.

This could be accomplished by directed evolution, the inclusion of a synthetic receptor, or the creation of a protein fusion with an analyte-binding protein. Proteins substituted with lanthanide complexes could be utilized for multimodal imaging, exploiting both magnetic and luminescent properties for MRI and fluorescence imaging with a single protein. Additionally, heme proteins substituted with artificial cofactors can serve as dual functional probes that combine imaging and therapeutic agents in a single construct. The examples detailed in this *Account* outline a unique, versatile approach to address biomedical problems and lay the foundation for the development of next-generation diagnostics and therapeutics.

Supplementary Material

Refer to Web version on PubMed Central for supplementary material.

Acknowledgments

This research was supported by a grant from the National Institutes of Health (NIH): R01GM127854. The members of the Marletta lab are graciously thanked for critically evaluating this manuscript.

Biographies

Christopher M. Lemon is a postdoctoral fellow with Prof. Michael Marletta at the University of California, Berkeley. He received a B.S. degree in biochemistry and physics and a B.A. degree in mathematical statistics form Ohio Northern University in 2008. He was then a Fulbright scholar at the University of Auckland in New Zealand. Lemon conducted his graduate studies at MIT (S.M., 2013) and then Harvard University (PhD, 2016). In 2016, he joined the Marletta lab as a Miller Fellow, developing designer heme proteins with novel function.

Michael A. Marletta is the CH and Annie Li Chair in the Molecular Biology of Diseases at the University of California, Berkeley. He received an A.B. degree in biology and chemistry from Fredonia, SUNY (1973), a PhD in 1978 from the University of California, San Francisco followed by postdoctoral studies at MIT. He has held faculty positions at MIT, the University of Michigan, and UC Berkeley. He was also an investigator of the Howard Hughes Medical Institute. He was president and CEO of the Scripps Research Institute and then returned to Berkeley in 2015. He is a member of the National Academy of Medicine, the American Academy of Arts and Sciences, and the National Academy of Sciences. Marletta's primary research interests lie at the interface of chemistry and biology with emphasis on the study of protein function and enzyme reaction mechanisms.

References

(1). Woodward JJ; Martin NI; Marletta MA An *Escherichia coli* Expression-Based Method for Heme Substitution. Nat. Methods 2007, 4, 43–45. [PubMed: 17187078] This paper describes the methodology and initial scope of expression-based incorporation of heme analogs bearing different metal centers and peripheral substituents in hemoproteins using the RP523 strain of *E. coli*.

(2). Winter MB; McLaurin EJ; Reece SY; Olea C; Nocera DG; Marletta MA Ru-Porphyrin Protein Scaffolds for Sensing O_2. J. Am. Chem. Soc 2010, 132, 5582–5583. [PubMed: 20373741] A ruthenium porphyrin is incorporated into myoglobin and *Cs* H-NOX for optical oxygen sensing

at biologically relevant O_2 concentrations. Phosphorescence from *Cs* H-NOX is higher than myoglobin, indicating that this protein is an ideal platform for developing photo-responsive proteins.

(3). Winter MB; Klemm PJ; Phillips-Piro CM; Raymond KN; Marletta MA Porphyrin-Substituted H-NOX Proteins as High-Relaxivity MRI Contrast Agents. Inorg. Chem 2013, 52, 2277–2279. [PubMed: 23394479] Manganese and gadolinium porphyrins are incorporated into *Cs* H-NOX to yield contrast agents for magnetic resonance imaging (MRI). These proteins exhibit higher relaxivities than clinically used small molecule contrast agents.

(4). Lemon CM; Marletta MA Corrole-Substituted Fluorescent Heme Proteins. Inorg. Chem 2021, 60, 2716–2729. [PubMed: 33513009] A fluorescent phosphorous corrole is incorporated into *Cs* H-NOX and *Pa* HasA. Both proteins exhibit enhanced fluorescence relative to the free, unbound corrole. The methodology for direct expression of apoproteins with the RP523 strain of *E. coli* is also described.

(5). Poulos TL Heme Enzyme Structure and Function. Chem. Rev 2014, 114, 3919–3962. [PubMed: 24400737]

(6). Liu X; Yu Y; Hu C; Zhang W; Lu Y; Wang J Significant Increase of Oxidase Activity through the Genetic Incorporation of a Tyrosine–Histidine Cross-Link in a Myoglobin Model of Heme–Copper Oxidase. Angew. Chem. Int. Ed 2012, 51, 4312–4316.

(7). Yu Y; Cui C; Liu X; Petrik ID; Wang J; Lu Y A Designed Metalloenzyme Achieving the Catalytic Rate of a Native Enzyme. J. Am. Chem. Soc 2015, 137, 11570–11573. [PubMed: 26318313]

(8). Yu Y; Lv X; Li J; Zhou Q; Cui C; Hosseinzadeh P; Mukherjee A; Nilges MJ; Wang J; Lu Y Defining the Role of Tyrosine and Rational Tuning of Oxidase Activity by Genetic Incorporation of Unnatural Tyrosine Analogs. J. Am. Chem. Soc 2015, 137, 4594–4597. [PubMed: 25672571]

(9). Mirts EN; Bhagi-Damodaran A; Lu Y Understanding and Modulating Metalloenzymes with Unnatural Amino Acids, Non-Native Metal Ions, and Non-Native Metallocofactors. Acc. Chem. Res 2019, 52, 935–944. [PubMed: 30912643]

(10). Hoffman BM; Petering DH Coboglobins: Oxygen-Carrying Cobalt-Reconstituted Hemoglobin and Myoglobin. Proc. Natl. Acad. Sci. U. S. A 1970, 67, 637–643. [PubMed: 4331717]

(11). Dierks EA; Hu S; Vogel KM; Yu AE; Spiro TG; Burstyn JN Demonstration of the Role of Scission of the Proximal Histidine–Iron Bond in the Activation of Soluble Guanylyl Cyclase through Metalloporphyrin Substitution Studies. J. Am. Chem. Soc 1997, 119, 7316–7323,

(12). Herzik MA; Jonnalagadda R; Kuriyan J; Marletta MA Structural Insights into the Role of Iron-Histidine Bond Cleavage in Nitric Oxide-Induced Activation of H-NOX Gas Sensor Proteins. Proc. Natl. Acad. Sci. U. S. A 2014, 111, E4156–E4164. [PubMed: 25253889]

(13). Natoli SN; Hartwig JF Noble–Metal Substitution in Hemoproteins: An Emerging Strategy for Abiological Catalysis. Acc. Chem. Res 2019, 52, 326–335. [PubMed: 30693758]

(14). Oohora K; Onoda A; Hayashi T Hemoproteins Reconstituted with Artificial Metal Complexes as Biohybrid Catalysts. Acc. Chem. Res 2019, 52, 945–954. [PubMed: 30933477]

(15). Huang P-S; Boyken SE; Baker D The Coming of Age of de novo Protein Design. Nature 2016, 537, 320–327. [PubMed: 27629638]

(16). Robertson DE; Farid RS; Moser CC; Urbauer JL; Mulholland SE; Pidikiti R; Lear JD; Wand AJ; DeGrado WF; Dutton PL Design and Synthesis of Multi-Haem Proteins. Nature 1994, 368, 425–432. [PubMed: 8133888]

(17). Cochran FV; Wu SP; Wang W; Nanda V; Saven JG; Therien MJ; DeGrado WF Computational De Novo Design and Characterization of a Four-Helix Bundle Protein that Selectively Binds a Nonbiological Cofactor. J. Am. Chem. Soc 2005, 127, 1346–1347. [PubMed: 15686346]

(18). Anderson JLR; Armstrong CT; Kodali G; Lichtenstein BR; Watkins DW; Mancini JA; Boyle AL; Farid TA; Crump MP; Moser CC; Dutton PL Constructing a Man-Made c-Type Cytochrome Maquette *in vivo*: Electron Transfer, Oxygen Transport and Conversion to a Photoactive Light Harvesting Maquette. Chem. Sci 2014, 5, 507–514. [PubMed: 24634717]

(19). Kodali G; Mancini JA; Solomon LA; Episova TV; Roach N; Hobbs CJ; Wagner P; Mass OA; Aravindu K; Barnsley JE; Gordon KC; Officer DL; Dutton PL; Moser CC Design and Engineering of Water-Soluble Light-Harvesting Protein Maquettes. Chem. Sci 2017, 8, 316–324. [PubMed: 28261441]

(20). Sheehan MM; Magaraci MS; Kuznetsov IA; Mancini JA; Kodali G; Moser CC; Dutton PL; Chow BY Rational Construction of Compact de Novo-Designed Biliverdin-Binding Proteins. Biochemistry 2018, 57, 6752–6756. [PubMed: 30468389]

(21). Sharp RE; Diers JR; Bocian DF; Dutton PL Differential Binding of Iron(III) and Zin(II) Protoporphyrin IX to Synthetic Four-Helix Bundles. J. Am. Chem. Soc 1998, 120, 7103–7104.

(22). Fry HC; Lehmann A; Saven JG; DeGrado WF; Therien MJ Computational Design and Elaboration of a de Novo Heterotetrameric α-Helical Protein That Selectively Binds an Emissive Abiological (Porphinato)zinc Chromophore. J. Am. Chem. Soc 2010, 132, 3997–4005. [PubMed: 20192195]

(23). Guo Y; Marletta MA Structural Insight into H-NOX Gas Sensing and Cognate Signaling Protein Regulation. ChemBioChem 2019, 20, 7–19. [PubMed: 30320963]

(24). Horst BG; Marletta MA Physiological Activation and Deactivation of Soluble Guanylate Cyclase. Nitric Oxide 2018, 77, 65–74. [PubMed: 29704567]

(25). Wittenborn EC; Marletta MA Structural Perspectives on the Mechanism of Soluble Guanylate Cyclase Activation. Int. J. Mol. Sci 2021, 22, 5439. [PubMed: 34064029]

(26). Contreras H; Chim N; Credali A; Goulding CW Heme Uptake in Bacterial Pathogens. Curr. Opin. Chem. Biol 2014, 19, 34–41. [PubMed: 24780277]

(27). Jepkorir G; Rodríguez JC; Rui H; Im W; Lovell S; Battaile KP; Alontaga AY; Yukl ET; Moënne-Loccoz P; Rivera M Structural, NMR Spectroscopic, and Computational Investigation of Hemin Loading in the Hemophore HasAp from Pseudomonas aeruginosa. J. Am. Chem. Soc 2010, 132, 9857–9872. [PubMed: 20572666]

(28). Arnoux P; Haser R; Izadi-Pruneyre N; Lecroisey A; Czjzek M Functional Aspects of the Heme Bound Hemophore HasA by Structural Analysis of Various Crystal Forms. Proteins 2000, 41, 202–210 [PubMed: 10966573]

(29). Létoffé S; Nato F; Goldberg ME; Wandersman C Interactions of HasA, a Bacterial Haemophore, with Haemoglobin and with Its Outer Membrane Receptor HasR. Mol. Microbol 1999, 33, 546–555.

(30). Vogel KM; Hu Z; Spiro TG; Dierks EA; Yu AE; Burstyn JN Variable Forms of Soluble Guanylyl Cyclase: Protein-Ligand Interactions and the Issue of Activation by Carbon Monoxide. J. Biol. Inorg. Chem 1999, 4, 804–813. [PubMed: 10631613]

(31). Denninger JW; Schelvis JPM; Brandish PE; Zhao Y; Babcock GT; Marletta MA Interaction of Soluble Guanylate Cyclase with YC-1: Kinetic and Resonance Raman Studies. Biochemistry 2000, 39, 4191–4198. [PubMed: 10747811]

(32). Copper corroles exhibit ligand non-innocence. Consequently, the ground state electronic structure of these molecules is best described as an antiferromagnetically coupled Cu(II) corrole radical cation: Lemon CM; Huynh M; Maher AG; Anderson BL; Bloch ED; Powers DC; Nocera DG Electronic Structure of Copper Corroles. Angew. Chem. Int. Ed 2016, 55, 2176–2180.

(33). Li J-M; Umanoff H; Proenca R; Russell CS; Cosloy SD Cloning of the *Escherichia coli* K-12 hemB Gene. J. Bacteriol 1988, 170, 1021–1025. [PubMed: 3276659]

(34). Winter MB; Woodward JJ; Marletta MA An *Escherichia coli* Expression-Based Approach for Porphyrin Substitution in Heme Proteins. In Cytochrome P450 Protocols, Methods in Molecular Biology; Phillips IR, Shepard EA, Ortiz de Montellano PR, Eds,; Humana Press: Totowa, NJ, 2013; Vol. 987; pp 95–106.

(35). Nierth A; Marletta MA Direct meso-Alkynylation of Metalloporphyrins through Gold Catalysis for Hemoprotein Engineering. Angew. Chem. Int. Ed 2014, 53, 2611–2614.

(36). Orłowski R; Gryko D; Gryko DT Synthesis of Corroles and Their Heteroanalogs. Chem. Rev 2017, 117, 3102–3137. [PubMed: 27813401]

(37). Barata JFB; Neves MGPMS; Faustino MAF; Tomé AC; Cavaleiro JAS Strategies for Corrole Functionalization. Chem. Rev 2017, 117, 3192–3253. [PubMed: 28222602]

(38). Ghosh A Electronic Structure of Corrole Derivatives: Insights from Molecular Structures, Spectroscopy, Electrochemistry, and Quantum Chemical Calculations. Chem. Rev 2017, 117, 3798–3881. [PubMed: 28191934]

(39). Alemayehu AB; Thomas KE; Einrem RF; Ghosh A The Story of 5d Metallocorroles: From Metal–Ligand Misfits to New Building Blocks for Cancer Phototherapeutics. Acc. Chem. Res 2021, 54, 3095–3107. [PubMed: 34297542]

(40). Lemon CM Corrole Photochemistry. Pure Appl. Chem 2020, 92, 1901–1919.

(41). Nardis S; Mandoj F; Stefanelli M; Paolesse T Metal Complexes of Corrole. Coord. Chem. Rev 2019, 388, 360–405.

(42). Brugna M; Tasse L; Hederstedt L *In vivo* Production of Catalase Containing Haem Analogues. FEBS J. 2010, 277, 2663–2672. [PubMed: 20553500]

(43). Lelyveld VS; Brustad E; Arnold FH; Jasanoff A Metal-Substituted Protein MRI Contrast Agents Engineered for Enhanced Relaxivity and Ligand Sensitivity. J. Am. Chem. Soc 2011, 133, 649–651. [PubMed: 21171606]

(44). Perkins LJ; Weaver BR; Buller AR; Burstyn JN De novo Biosynthesis of a Nonnatural Cobalt Porphyrin Cofactor in *E. coli* and Incorporation into Hemoproteins. Proc. Natl. Acad. Sci. U.S.A 2021, 118, e2017625118. [PubMed: 33850014]

(45). Roussakis E; Li Z; Nichols AJ; Evans CL Oxygen-Sensing Methods in Biomedicine from the Macroscale to the Microscale. Angew. Chem. Int. Ed 2015, 54, 8340–8362.

(46). Wang X-D; Wolfbeis OS Optical Methods for Sensing and Imaging Oxygen: Materials, Spectroscopies and Applications. Chem. Soc. Rev 2014, 43, 3666–3761. [PubMed: 24638858]

(47). Lemon CM Optical Oxygen Sensing with Quantum Dot Conjugates. Pure Appl. Chem 2018, 90, 1359–1377.

(48). Cowan JA; Gray HB Synthesis and Properties of Metal-Substituted Myoglobins. Inorg. Chem 1989, 28, 2074–2078.

(49). Vanderkooi JM; Wright WW; Erecinska M Oxygen Gradients in Mitochondria Examined with Delayed Luminescence from Excited-State Triplet Probes. Biochemistry 1990, 29, 5332–5338. [PubMed: 2383550]

(50). Nibbs J; Vinogradov SA; Vanderkooi JM; Zelent B Flexibility in Proteins: Tuning the Sensitivity to O_2 Diffusion by Varying the Lifetime of a Phosphorescent Sensor in Horseradish Peroxidase. Photochem. Photobiol 2004, 80, 36–40. [PubMed: 15339214]

(51). Lemon CM; Curtin PN; Somers RC; Greytak AB; Lanning RM; Jain RK; Bawendi MG; Nocera DG Metabolic Tumor Profiling with pH, Oxygen, and Glucose Chemosensors on a Quantum Dot Scaffold. Inorg. Chem 2014, 53, 1900–1915. [PubMed: 24143874]

(52). Caravan P; Ellison JJ; McMurry TJ; Lauffer RB Gadolinium(III) Chelates as MRI Contrast Agents: Structure, Dynamics, and Applications. Chem. Rev 1999, 99, 2293–2352. [PubMed: 11749483]

(53). Wahsner J; Gale EM; Rodríguez-Rodríguez A; Caravan P Chemistry of MRI Contrast Agents: Current Challenges and New Frontiers. Chem. Rev 2019, 119, 957–1057. [PubMed: 30350585]

(54). Shapiro MG; Westmeyer GG; Romero PA; Szablowski JO; Küster B; Shah A; Otey CR; Langer R; Arnold FH; Jasanoff A Directed Evolution of a Magnetic Resonance Imaging Contrast Agent for Noninvasive Imaging of Dopamine. Nat. Biotechnol 2010, 28, 264–270. [PubMed: 20190737]

(55). Li Y; Drummond DA; Sawayama AM; Snow CD; Bloom JD; Arnold FH A Diverse Family of Thermostable Cytochrome P450s Created by Recombination of Stabilizing Fragments. Nat. Biotechnol 2007, 25, 1051–1056. [PubMed: 17721510]

(56). Ventola CL The Antibiotic Resistance Crisis Part 1: Causes and Threats. Pharm. Ther 2015, 40, 277–283.

(57). Blair JM; Webber MA; Baylay AJ; Ogbolu DO; Piddock LJV Molecular Mechanisms of Antibiotic Resistance. Nat. Rev. Microbiol 2015, 13, 42–51. [PubMed: 25435309]

(58). Ventola CL The Antibiotic Resistance Crisis Part 2: Management Strategies and New Agents. Pharm. Ther 2015, 40, 344–352.

(59). Brown ED; Wright GD Antibacterial Drug Discovery in the Resistance Era. Nature 2016, 529, 336–343. [PubMed: 26791724]

(60). Cassat JE; Skaar EP Iron in Infection and Immunity. Cell Host Microbe 2013, 13, 509–519. [PubMed: 23684303]

(61). Shirataki C; Shoji O; Terada M; Ozaki S; Sugimoto H; Shiro Y; Watanabe Y Inhibition of Heme Uptake in Pseudomonas aeruginosa by its Hemophore (HasAp) Bound to Synthetic Metal Complexes. Angew. Chem. Int. Ed 2014, 53, 2862–2866.

(62). Shisaka Y; Iwai Y; Yamada S; Uehara H; Tosha T; Sugimoto H; Shiro Y; Stanfield JK; Ogawa K; Watanabe Y; Shoji O Hijacking the Heme Acquisition System of Pseudomonas aeruginosa for the Delivery of Phthalocyanine as an Antimicrobial. ACS Chem. Biol 2019, 14, 1637–1642. [PubMed: 31287285]

(63). Centola G; Deredge DJ; Hom K; Ai Y; Dent AT; Xue F; Wilks A Gallium(III)–Salophen as a Dual Inhibitor of Pseudomonas aeruginosa Heme Sensing and Iron Acquisition. ACS Infect. Dis 2020, 6, 2073–2085. [PubMed: 32551497]

(64). Chudakov DM; Matz MV; Lukyanov S; Lukyanov KA Fluorescent Proteins and Their Applications in Imaging Living Cells and Tissues. Physiol. Rev 2010, 90, 1103–1163. [PubMed: 20664080]

(65). König K Multiphoton Microscopy in Life Sciences. J. Microsc 2000, 200, 83–104. [PubMed: 11106949]

(66). Chu J; Xing Y; Lin MZ Far-Red and Near-Infrared Fluorescent Proteins. In The Fluorescent Protein Revolution; Day RN, Davidson MW, Eds,; CRC Press: Boca Raton, FL, 2014; pp 157–174.

(67). Aviv-Harel I; Gross Z Coordination Chemistry of Corroles with Focus on Main Group Elements. Coord. Chem. Rev 2011, 255, 717–736.

(68). Lemon CM; Nissley AJ; Latorraca NR; Wittenborn EC; Marletta MA Corrole–Protein Interactions in H-NOX and HasA. Submitted.

(69). Hespen CW; Bruegger JJ; Phillips-Piro CM; Marletta MA Structural and Functional Evidence Indicates Selective Oxygen Signaling in Caldanaerobacter subterraneus H-NOX. ACS Chem. Biol 2016, 11, 2337–2346. [PubMed: 27328180]

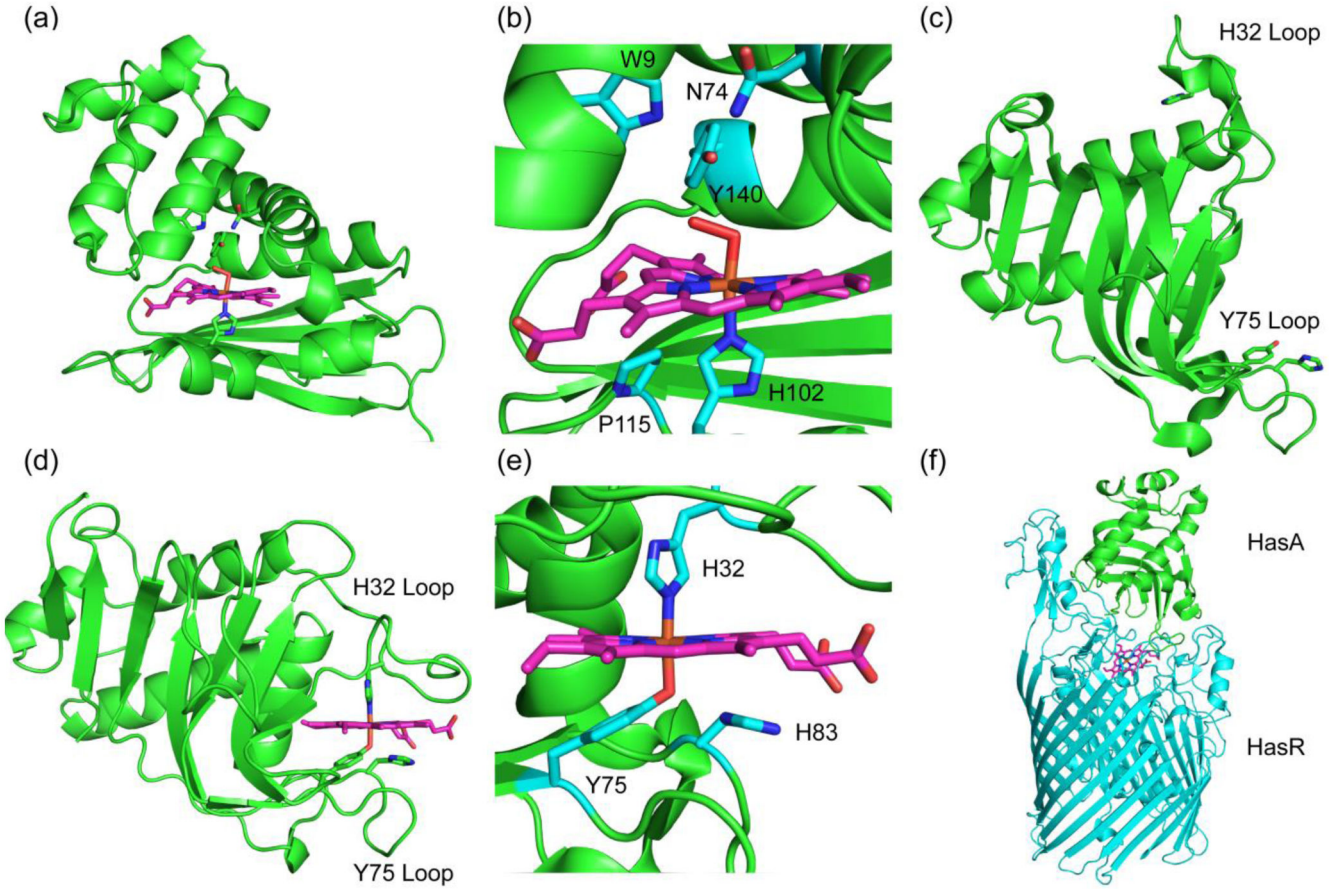

Figure 1.

(a) Crystal structure of the Fe(II)–O_2 complex of *Cs* H-NOX (PDB: 3TF0). (b) The heme binding pocket of *Cs* H-NOX highlighting key residues in cyan. (c) Crystal structure of the apo form of *Pa* HasA (PDB: 3MOK). (d) Crystal structure of the holo form of *Pa* HasA (PDB: 3ELL). (e) The heme binding pocket of *Pa* HasA highlighting key residues in cyan. (f) HasA (green) in complex with HasR (cyan) and heme from *Serratia marcescens* (PDB: 3CSL).

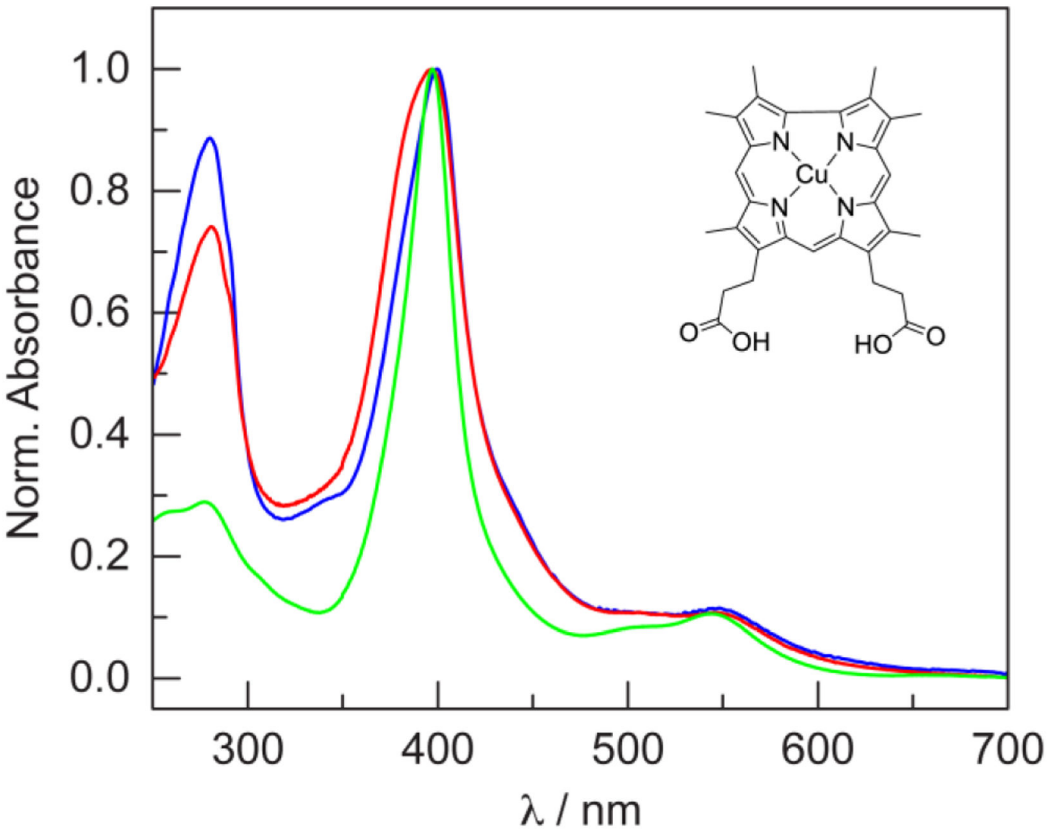

Figure 2.

Normalized absorption spectra of a copper corrole incorporated into *Cs* H-NOX via reconstitution (▬) or RP523 expression (▬) versus the free corrole methyl ester in $CHCl_3$ (▬). See Table S1 for numerical data. The different Soret bands for the protein samples reflect distinct binding modes of the corrole cofactor.

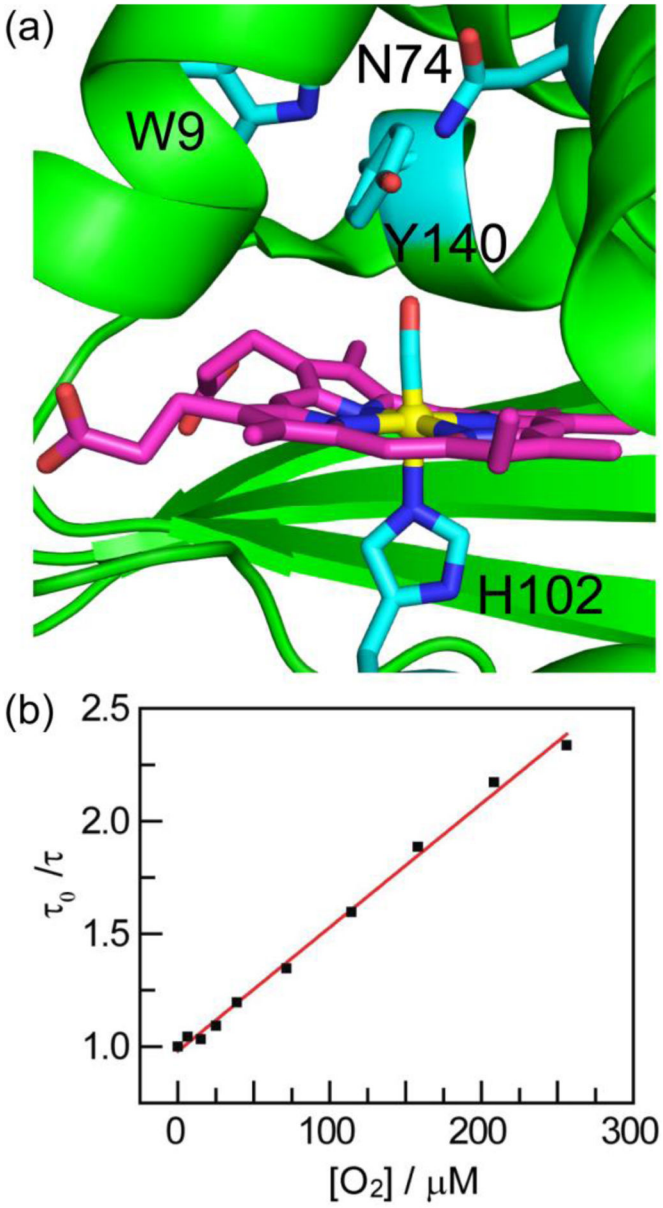

Figure 3.

(a) Heme binding pocket of *Cs* H-NOX with bound Ru(CO)(MPIX) (PDB: 3M0B). (b) Stern–Volmer plot for the Ru-substituted H-NOX depicting the phosphorescence lifetime as a function of oxygen concentration. Reprinted with permission from Ref. 2. Copyright 2010 American Chemical Society.

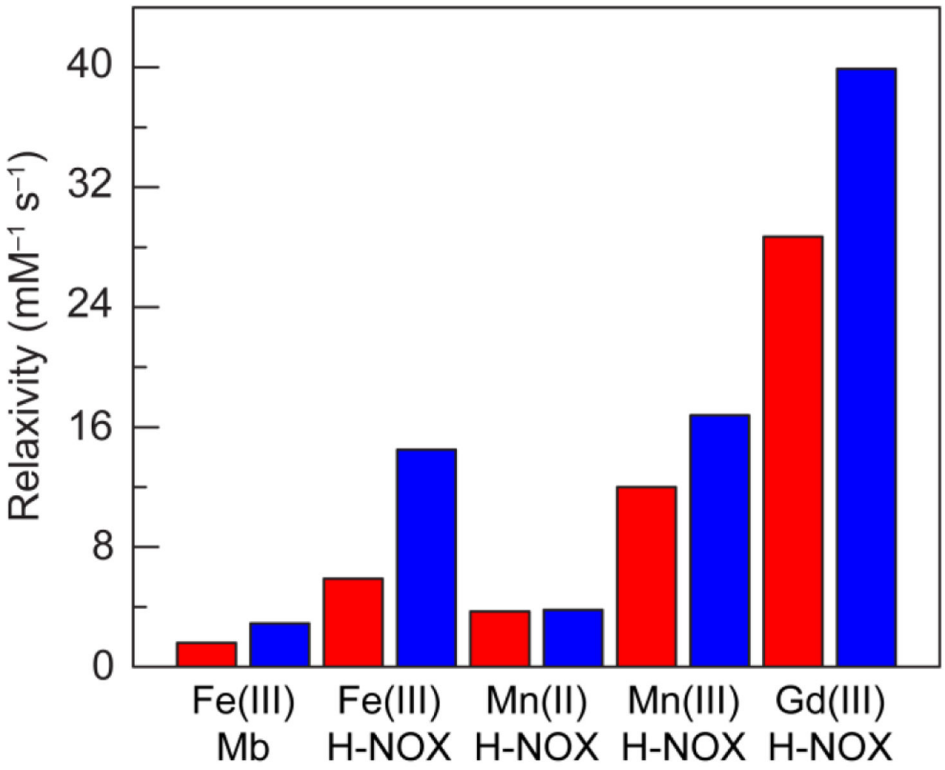

Figure 4.
Relaxivity of heme proteins (myoglobin (Mb) or H-NOX) substituted with various metalloporphyrins; r_1 in red bars, r_2 in blue bars.

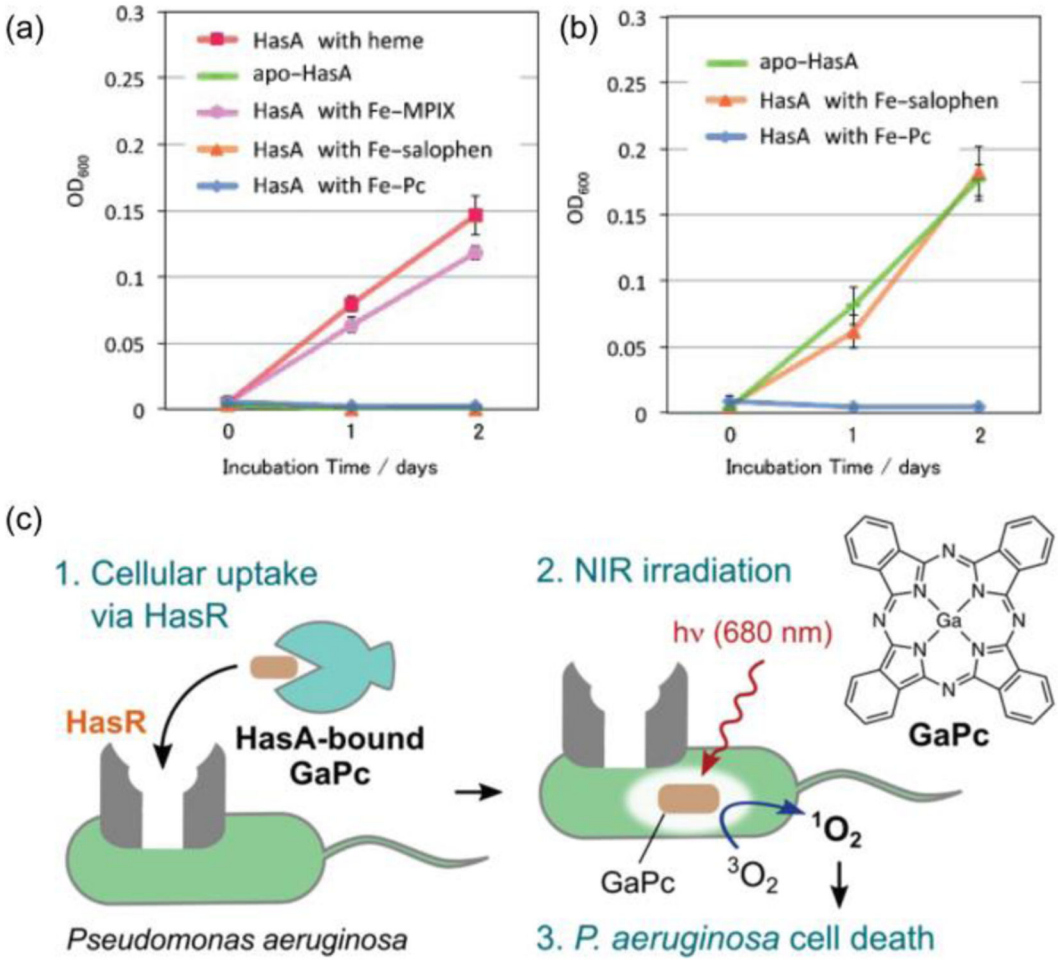

Figure 5.

(a) Effect of *Pa* HasA substituted with various Fe cofactors on the growth of *P. aeruginosa*. (b) Growth curves of *P. aeruginosa* cultured in the presence of both heme-loaded HasA (as an iron source) and substituted HasA, indicating that Fe phthalocyanine blocks heme uptake. Adapted with permission from Ref. 61. Copyright 2014 Wiley-VCH Verlag GmbH & Co. KGaA. (c) Schematic representation of the photochemical inactivation of *P. aeruginosa* using HasA substituted with Ga phthalocyanine. Adapted with permission from Ref. 62. Copyright 2019 American Chemical Society.

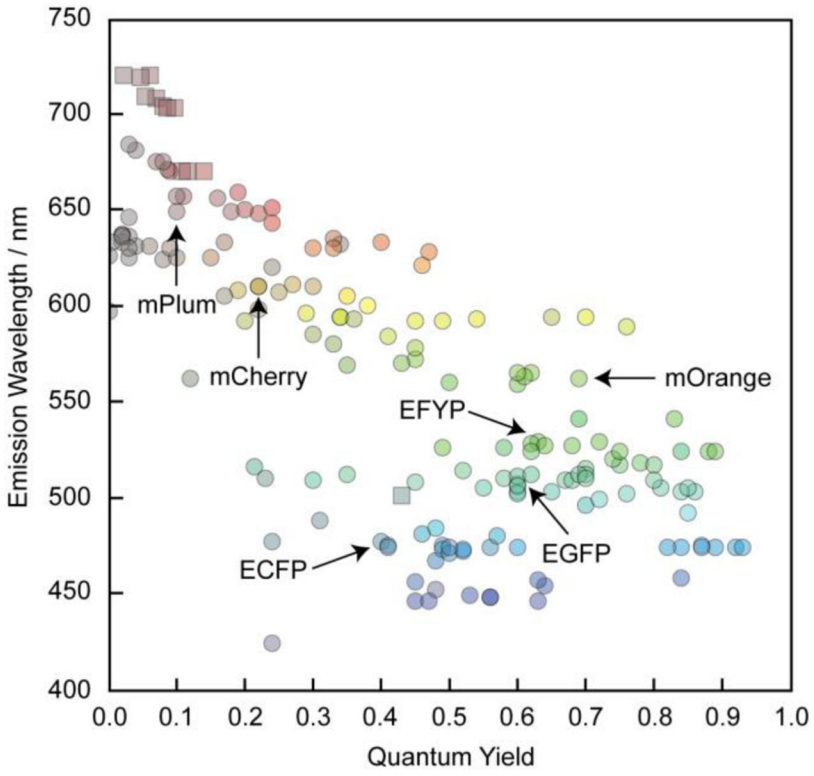

Figure 6.

A plot of the emission maximum versus fluorescence quantum yield for traditional fluorescent proteins. Spectral data was obtained from the online fluorescent protein database FPbase (fpbase.org).

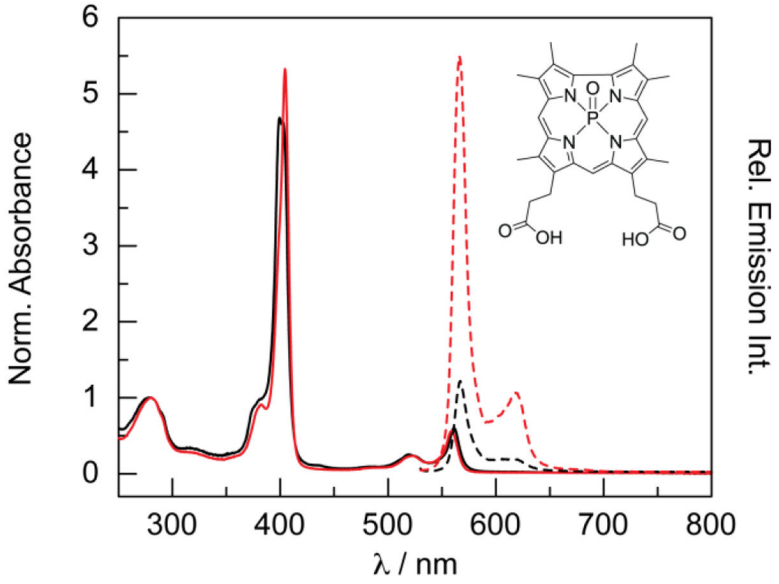

Figure 7.

Comparison of the absorption (solid lines) and emission spectra (dashed lines) of H-NOX (▬) and HasA (▬) with P=O corrole. The emission spectra of absorbance-matched samples reflect the difference in ϕ_f. See Table S2 for numerical data. Adapted with permission from Ref. 4. Copyright 2021 American Chemical Society.

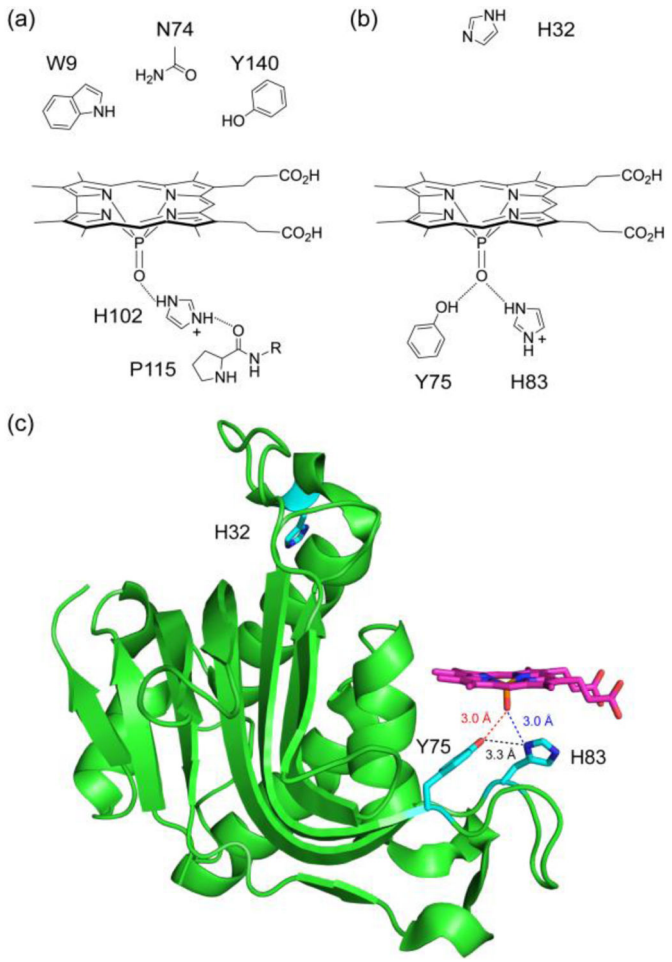

Figure 8.

Proposed models for P=O corrole binding in (a) *Cs* H-NOX and (b) *Pa* HasA. In both cases, the critical interaction is a hydrogen bond between the P=O unit and a protonated histidine side chain. (c) Docking model between P=O corrole and apo HasA (PDB: 3MOK).

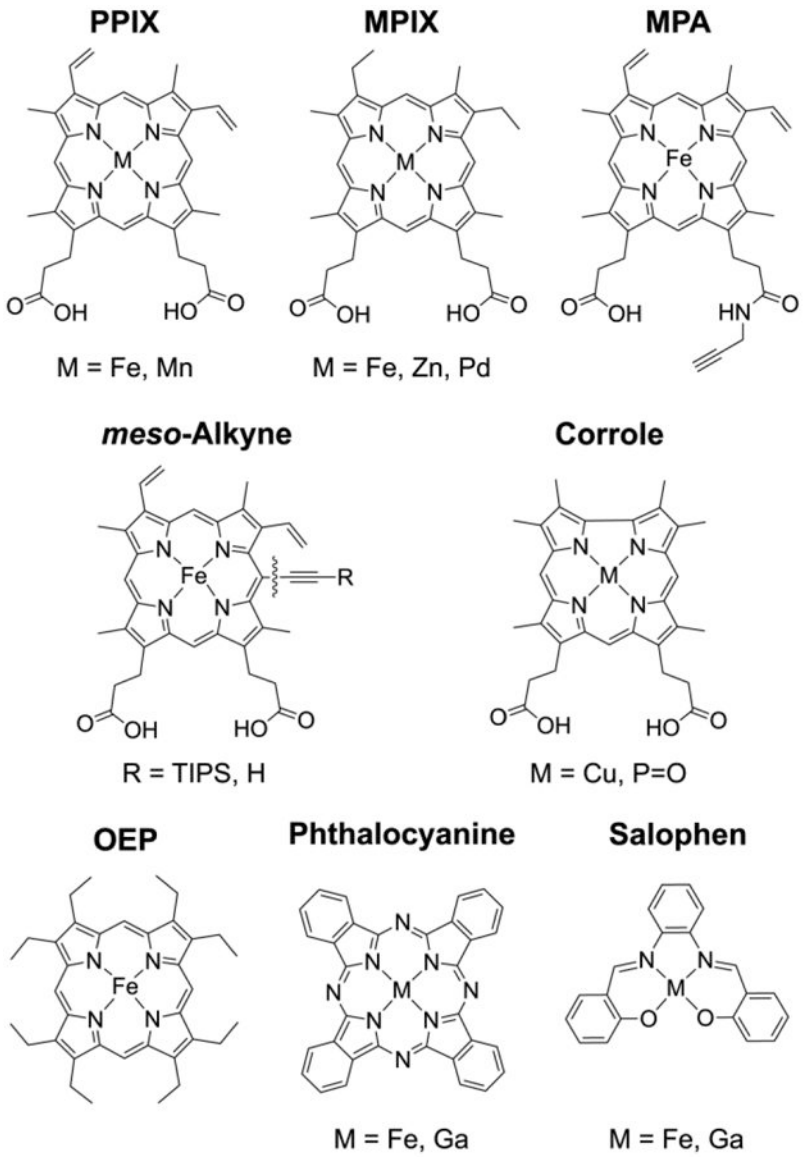

Chart 1.

Cofactors incorporated into H-NOX and HasA: PPIX = protoporphyrin IX, MPIX = mesoporphyrin IX, MPA = monopropargylamide, OEP = octaethylporphyrin.